

Gold coating of micromechanical DNA biosensors by pulsed laser deposition

Esther Rebollar, Mikel Sanz, Carina Esteves, Nicolás F. Martínez, Óscar Ahumada et al.

Citation: *J. Appl. Phys.* **112**, 084330 (2012); doi: 10.1063/1.4761986

View online: <http://dx.doi.org/10.1063/1.4761986>

View Table of Contents: <http://jap.aip.org/resource/1/JAPIAU/v112/i8>

Published by the [American Institute of Physics](http://www.aip.org).

Related Articles

Low-temperature indium-bonded alkali vapor cell for chip-scale atomic clocks
J. Appl. Phys. **113**, 064501 (2013)

Multi-layered dielectric cladding plasmonic microdisk resonator filter and coupler
Phys. Plasmas **20**, 020701 (2013)

Micromachined piezoelectric microphones with in-plane directivity
Appl. Phys. Lett. **102**, 054109 (2013)

Referee acknowledgment for 2012
Biomicrofluidics **7**, 010201 (2013)

Introducing a well-ordered volume porosity in 3-dimensional gold microcantilevers
Appl. Phys. Lett. **102**, 053501 (2013)

Additional information on J. Appl. Phys.

Journal Homepage: <http://jap.aip.org/>

Journal Information: http://jap.aip.org/about/about_the_journal

Top downloads: http://jap.aip.org/features/most_downloaded

Information for Authors: <http://jap.aip.org/authors>

ADVERTISEMENT



AIP Advances

Now Indexed in Thomson Reuters Databases

Explore AIP's open access journal:

- Rapid publication
- Article-level metrics
- Post-publication rating and commenting

Gold coating of micromechanical DNA biosensors by pulsed laser deposition

Esther Rebollar,^{1,a)} Mikel Sanz,¹ Carina Esteves,² Nicolás F. Martínez,² Óscar Ahumada,² and Marta Castillejo¹

¹*Instituto de Química Física Rocasolano, CSIC, Serrano 119, 28006 Madrid, Spain*

²*Mecwins, Santiago Grisolia 2 (PTM), Tres Cantos, 28760 Madrid, Spain*

(Received 6 June 2012; accepted 3 October 2012; published online 25 October 2012)

In this work, we describe the gold-coating of silicon microcantilever sensors by pulsed laser deposition (PLD) and their performance as DNA biosensors. To test optimum deposition conditions for coating the sensors, silicon substrates were gold coated by PLD using the fifth harmonic of a Nd:YAG laser (213 nm, pulse duration 15 ns). The gold deposits were characterized by atomic force microscopy and x-ray diffraction. The adequate conditions were selected for coating the sensors with a 20 nm thick gold layer and subsequently functionalized with a self-assembled monolayer of thiolated DNA. To verify PLD as a tool for gold coating of biomechanical sensors, they were characterized by using a scanning laser analyzer platform. Characterization consisted in the measurement of the differential stress of the cantilevers upon hydration forces before and after functionalization with a double-stranded DNA monolayer. The measurements showed that the sensor surface stress induced by the adsorption of water molecules is approximately seven times higher than that of functionalized sensors gold coated by thermal evaporation. These results indicate that gold coating by PLD could be an advantageous method to enhance the response of biomechanical sensors based on gold-thiol chemistry. © 2012 American Institute of Physics. [<http://dx.doi.org/10.1063/1.4761986>]

I. INTRODUCTION

Nanostructured materials and surfaces have generated great interest in recent years due to their unusual optical, electronic, magnetic, and catalytic properties.¹ Gold nanoparticles are used in optoelectronics, communications, chemical and electrochemical sensors, biosensors, etc.^{2–7} Surface parameters, like microstructure and morphology, normal electrochemical potential, surface energy, absorption, and reflection coefficients, play a vital role in determining the use of the deposited thin films or nanostructures made of gold. Pulsed laser deposition (PLD) has emerged as an attractive technique for the fabrication of well-defined nanostructures and surface morphologies of various materials because of the ability to control the dimensions and the crystalline phase by varying the laser parameters and the deposition conditions.^{8–13} This technique also offers the capability for producing epitaxial growth, and it has extensively been applied to produce metal nanoparticles.¹⁴

Mechanical biosensors are based on the principle that molecular recognition on the surface of a bio-functionalized micromechanical system (e.g., a cantilever) can result in a bending (deflection) of a few nanometers. The origin of the nanomechanical response is the change of the surface stress due to electrostatic, van der Waals, and steric intermolecular interactions on the cantilever surface.¹⁵ These devices require the binding of the molecules on only one side of the cantilever, which is achieved by coating it with a thin gold layer. The gold layer is then functionalized with the receptors by means of thiol chemistry. Previous research¹⁶ has shown that silicon microcantilevers gold coated by thermal

evaporation on one side experience a measurable bending in response to temperature changes, in a phenomenon referred as "bimetallic effect." The differential stress in the bimaterial cantilever is created due to dissimilar thermal expansion coefficients of the silicon substrate and the gold coating.

Self-assembled monolayers (SAMs) of single-stranded DNA (ssDNA) probes immobilized on solid supports constitute the base of a variety of biosensors.^{17,18} There is an increasing interest in using micromechanical sensors functionalized with SAMs of DNA to detect complementary DNA sequence with high sensitivity and specificity. In this type of sensors, a gold layer of few nanometers is used as an intermediate layer between the surface of the mechanical sensor and DNA. The features of the gold layer are crucial for the performance of the mechanical sensor. In particular, the surface of the gold film has to induce the creation of a high density SAM, while the bulk has to transmit the overall change of the surface tension to the mechanical sensor when complementary DNA chains are detected. The goal of a biosensor is the measurement of interactions between molecules; however, the forces involved are rather weak and closely related to the typically aqueous medium where they act. It has been shown¹⁷ that it is possible to take advantage of the leverage of hydration forces in controlled bilayers to produce magnified responses of micromechanical sensors. This provides a way to detect DNA hybridization with improved sensitivity and larger reproducibility and robustness in the response.¹⁷

In this work, we describe the gold-coating of silicon cantilever sensors by PLD and characterize their performance as DNA biosensors. PLD experiments were first carried out on silicon substrates in order to identify the optimum deposition conditions for coating the sensors. As excitation

^{a)}E-mail: e.rebollar@iqfr.csic.es.

source we used the fifth harmonic of a Q-switched Nd:YAG laser, delivering 15 ns pulses at 213 nm. The resulting nanostructured gold deposits were characterized by atomic force microscopy (AFM) and x-ray diffraction (XRD). A 20 nm thick gold layer was chosen as optimum for coating the micromechanical sensors and their differential stress, in response to temperature changes was characterized by using a scanning laser analyzer (SCALA).^{19,20} We analyzed the performance of the gold-coated micromechanical sensors in comparison to those fabricated by the conventional method of thermal evaporation used in previous work.¹⁷ For that purpose, we measured the mechanical response upon hydration, before and after the adsorption of self-assembled double-stranded DNA (dsDNA) monolayers. The results obtained indicate an improvement of the sensitivity of the biosensors prepared by using the PLD procedure.

II. EXPERIMENTAL

A. Preparation and characterization of gold films by PLD

The PLD set up consists of a stainless-steel chamber pumped down to 6×10^{-5} Pa by a turbo-molecular pump.¹¹ The gold targets (99.99% purity; Quorum Technologies, Kent, UK) were placed on a rotating sample holder to avoid cratering during repetitive irradiation. Deposits were prepared in vacuum using a Q-switched Nd:YAG (Lotis TII LS-2147) operating at 213 nm (5th harmonic of the fundamental radiation, full width half maximum (FWHM) 15 ns), at a repetition rate of 10 Hz. The laser beam was focused on the target surface by a 25 cm focal length lens to yield fluences up to 2 J/cm^2 . Prior to coating the silicon cantilevers, the optimum conditions for depositing a nanostructured gold thin film layer were identified by fabricating deposits on a silicon substrate. The silicon substrates (MikroMasch, Tallinn, Estonia) of ca. $1 \times 1 \text{ cm}^2$ were previously coated with an intermediate 2 nm thick chromium layer by sputtering (in a Emitech K575X Sputter Coater, Quorum Technologies, Kent, UK) in order to enhance the adhesion between the gold layer and the silicon substrate. The chromium-coated silicon substrates were placed at a distance of 4 cm from the ablation target. Deposits were grown at room temperature by delivering different number of pulses, up to 144 000, to the gold target resulting in deposition times of up to 4 h. Examination of the surface of the deposits was carried out by AFM (Nanoscope III A Multimode, Veeco). Their crystallinity was studied by XRD (Philips XPert) using the Cu K α (1.54 Å) radiation in the $\theta/2\theta$ configuration.

As micromechanical sensors, commercially available silicon cantilever arrays from MikroMasch were used. The cantilevers are rectangular, and their nominal dimensions are 400 μm in length, 100 μm in width, and 1 μm in thickness, and feature a resonance frequency of $8 \pm 3 \text{ kHz}$ and a spring constant of 0.055 N/m. The silicon micromechanical sensor arrays were also coated by sputtering with a 2 nm chromium layer, and their whole surface was then covered by PLD with a gold layer of 20 nm by introducing them into the deposition chamber. The surface topography of the gold-coated sensors was also characterized by AFM (Nanoscope V Multimode,

Veeco Instruments Inc.) and their mechanical response to temperature variations by using a SCALA device (Mecwins S.L., Madrid, Spain), a platform capable of fast deflection sensing and full 3D characterization of micromechanical sensors of any size.^{19,20} During these experiments, the temperature was changed at a rate of about 0.14°C per minute, and the relative humidity (RH) was kept at 0%.

B. Immobilization of DNA-SAM and measurement of the surface stress of the micromechanical sensors

The gold-coated micromechanical sensors were incubated with a $5 \mu\text{M}$ 5' thiol-modified ssDNA (5'-CTA CCT TTT TTT TCTG-3') (Microsynth, Balgach, Switzerland) probe in PBS solution (1.137 M NaCl, 0.003 M KCl, 0.008 M Na₂HPO₄, 0.002 M KH₂PO₄) for 258 h at 24 °C. Following the immobilization procedure, the sensors were vigorously rinsed in Milli-Q water, at room temperature to discard unspecific interactions, and were dried under dry nitrogen flow. Hybridization with ssDNA complementary strand (5'-CAG AAA AAA AAG GTAG-3') (Microsynth) was performed in PBS for 1 h at room temperature. They were rinsed afterwards and dried following the same protocol as described above.

The mechanical response (surface stress variations) of the gold-coated sensors to hydration forces was also measured by using the SCALA platform. Control of hydration forces was made by increasing the RH in the measurement chamber. During the measurement of the surface stress, the temperature was kept at 24 °C, and the RH was changed at a rate of about 1% per minute from 0% to 40%-50%. Before the measurement, the sensors were equilibrated at 0% RH in a flow of dry nitrogen for about 20 min.

To calculate the surface stress, σ , the SCALA platform performs a read-out of the cantilever deflection profiles, and each profile is fitted to a second order polynomial to deduce the curvature radius, R , as described in Ref. 16. The surface stress σ is related to R by the Stoney's equation²¹

$$\sigma = \frac{E}{6(1-\nu)} \frac{T^2}{R}, \quad (1)$$

where E and ν are, respectively, the Young's modulus and the Poisson coefficient of silicon (typically 169 GPa and 0.27, respectively)¹⁷ and T is the thickness of the cantilever. This calculation is performed continuously so that changes in R (and subsequently in the surface stress) can be monitored as the temperature or the RH conditions change.

III. RESULTS

A. Fabrication and characterization of coated substrates

The thickness of the deposits was measured by AFM and the values for different number of pulses are reported in Table I. As expected, the thickness increases upon repetitive irradiation of the target. The superficial nanostructure of the deposits was investigated by AFM. Figure 1 shows corresponding AFM height images. For a low number of pulses

TABLE I. Thickness and roughness (R_a) of the gold deposits prepared by PLD at the different irradiation conditions.

Number of pulses	Thickness(nm)	R_a (nm)
3000	...	1.5 ± 0.2
6000	...	1.5 ± 0.1
12 000	3 ± 1	0.3 ± 0.2
18 000	8 ± 2	0.4 ± 0.2
24 000	13 ± 2	0.7 ± 0.2
144 000	20 ± 3	0.8 ± 0.2

(up to 6000), the deposits are constituted by a nanoparticle-assembled layer with characteristic sizes from some tens up to 300 nm. However, for a higher number of pulses ($\geq 12\,000$), the grown films are continuous. The mean roughness values, R_a , obtained by calculating the arithmetic average of the height deviations from the centre plane of the sample are also listed in Table I. It is observed that the layer grown with 12 000 pulses presents a lower roughness than that grown with 6000 pulses, indicating the transition from a nanoparticle-assembled layer to a continuous film. For even larger number of pulses, R_a increases again as a consequence of the presence of large overimposed aggregates, which are evident in Figure 1.

As outcome of previous investigations,^{16,22,23} it is known that the adequate performance of the DNA biomechanical sensors requires the coverage of the cantilever surface by a thick enough gold layer of about 20 nm. In order to ensure that the gold layer grown by PLD meets this requirement, gold deposition was carried out using 144 000 laser pulses (Table I). Before coating the cantilevers by PLD, we characterized the crystalline structure and composition of the deposits grown on silicon with 144 000 laser pulses and compared with those of the initial gold target by using XRD. Figure 2 shows XRD patterns of the gold target and of the deposit. For the gold target, XRD peaks located at 38.27° and 44.45° are readily assigned to the (111) and (200) reflections, respectively.

These peaks, together with reflections located at 64.49° , 77.65° , and 81.83° (not shown in the figure) and assigned to the (220), (311), and (222) phases respectively, correspond to the face-centered cubic structure of metallic gold (Joint Committee on Powder Diffraction Standards, PCDS, Card No. 04-0784). The diffraction pattern of the deposit obtained with 144 000 pulses displays the same peaks as the target, with a clear predominance of the (111) phase. The intense (111) peak gives indication of the preferential orientation of gold crystallites onto the substrate surface. Similar phase predominance was obtained²⁴ for gold thin films grown on glass substrates by ns PLD exciting at 248 nm and was discussed in connection with the velocity of arrival of the ejected species to the substrate, which plays a central role in determining the deposit crystalline structure. Highly energetic plasma species ejected from the target are easily thermalized and diffused upon arrival at the substrate which grows as a highly oriented nanostructured film.²⁴

The average crystalline domain size of deposits, D , was estimated using the Scherrer law, $D = 0.9 \lambda / B \cos \theta_B$, where λ is the x-ray wavelength (Cu $K_\alpha = 0.154$ nm) and B is the FWHM (in radians) of the diffraction peak. The obtained crystalline domain size (23 nm) is smaller than that of the target material (38 nm). Also, the XRD analysis indicates that typical crystalline sizes of deposits are of the order of the nanoparticle size derived from AFM imaging analysis of the deposited film (see Figure 1(f)), thus indicating that the observed nanostructures are likely to be single-crystalline particles.

B. Characterization of gold coated mechanical sensors

The surface topography of the gold-coated sensors was characterized by AFM. Figure 3 shows the topography image of a 20 nm thick gold layer deposited on the surface of a cantilever using 144 000 laser pulses. The surface exhibits a

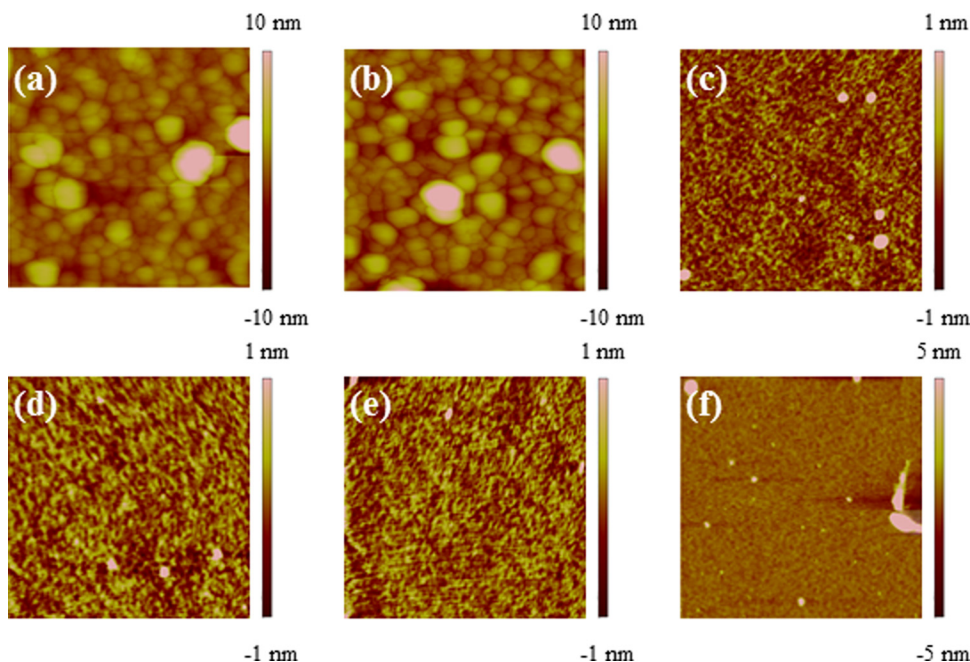


FIG. 1. AFM height images ($2 \times 2 \mu\text{m}^2$) of the surfaces of gold deposits obtained by PLD at 213 nm and 2 J/cm^2 after: (a) 3000, (b) 6000, (c) 12 000, (d) 18 000, (e) 24 000, and (f) 144 000 pulses.

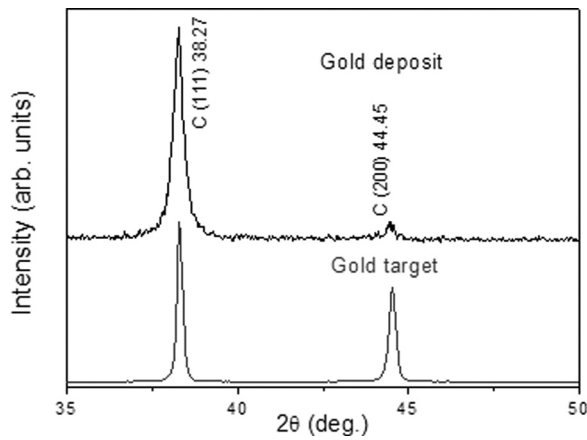


FIG. 2. XRD patterns of gold target and deposit grown by PLD at 213 nm and 2 J/cm^2 with 144 000 pulses.

well-defined continuous film with similar topography than the gold deposits prepared on the silicon substrate with the same number of pulses (Figure 1(f)). The measured surface roughness is 0.6 nm, which is consistent with the R_a value determined for the gold-coated substrates made by applying 144 000 laser pulses ($0.8 \pm 0.2 \text{ nm}$, Table I). The surface grain size is 20–24 nm, and the grain boundaries are well defined with a surface density of $523 \mu\text{m}^{-2}$. The coated surface also shows the deposition of larger aggregates, of grain size 34–38 nm, dispersed through the gold coating. These aggregates are present in a much lower density ($7 \mu\text{m}^{-2}$) in comparison to the small surface grains and are not connected; thus, they are not expected to play an important role on the transmission of surface stress.

The differential stress induced by the gold film on the surface of the cantilevers was characterized by measuring the mechanical response of the sensors to temperature variations. Figure 4 shows the vertical deflection of the free-end of two cantilevers within the same array (out of the 20 analyzed cantilevers in 4 different arrays of sensors) when submitted to temperature changes. With the increase of temperature, the cantilevers bend downwards toward the silicon side, due to the higher thermal expansion coefficient of gold as compared to that of silicon. The bimetallic coefficient dD/dT is obtained by linear fitting the thermal response of the cantilever. For the cantilevers shown in Figure 4, the values are $-47.6 \pm 0.4 \text{ nm}/^\circ\text{C}$ for cantilever 1 (squares) and $-72.5 \pm 0.5 \text{ nm}/^\circ\text{C}$ for cantilever 2 (circles). This difference is related with variations in the cantilever thickness in the

manufacturing process; in fact, it has been previously shown²⁵ that related variations over a factor of two could be expected for cantilevers made from the same silicon wafer. The bimetallic coefficient obtained by averaging measurements of the 20 tested cantilevers is $-51.54 \pm 15.36 \text{ nm}/^\circ\text{C}$. This experimental value can be compared with the theoretical prediction assuming a uniform continuous gold layer given by the expression²⁶

$$\frac{dD}{dT} = \frac{6E_c E_s (h_c + h_s) h_c h_s (\alpha_c - \alpha_s)}{E_c^2 h_c^4 + 4E_c E_s h_c^3 h_s + 6E_c E_s h_c^2 h_s^2 + 4E_c E_s h_c h_s^3 + E_s^2 h_s^4} \frac{L^2}{2}, \quad (2)$$

where L and h are the length and the thickness of the micro-mechanical sensor, α the thermal expansion coefficient, and the subscripts s and c refer to the substrate (silicon) and coating (gold layer), respectively. For simplicity, the chromium layer is neglected in this equation. Applying Eq. (2), a theoretical bimetallic coefficient value of $-46.3 \text{ nm}/^\circ\text{C}$ is obtained. This is in good agreement with the experimental one, indicating that the PLD method ensures a homogeneous coverage across the cantilever surface.

C. Assessment of micromechanical DNA biosensors

We assessed the performance of the functionalized cantilever sensors coated by PLD and compared it with that reported for the sensors coated by thermal evaporation.¹⁷ This was done by measuring the mechanical response under the influence of hydration forces after the adsorption of DNA molecules. The gold-coated cantilevers were incubated in a thiol-modified ssDNA solution followed by a hybridization procedure, as described in Sec. II. Thiol-modified ssDNA forms a SAM on the gold-coated side of the sensor due to the strong bond between the thiol group and gold.²³ At high packing conditions, DNA molecules align vertically, creating intermolecular sub-nanometric channels in which the confinement of water molecules changes the tension in the monolayer. DNA-DNA chain interactions of the monolayer through water molecules are transmitted to the gold surface modifying the surface stress of the cantilever sensor.¹⁷ The surface stress response to increasing hydration forces (i.e., increasing the RH) of the functionalized cantilever generates a characteristic response as described in Ref. 17.

Figure 5 shows the evolution of the surface stress upon hydration for the five cantilevers of one of the four analyzed

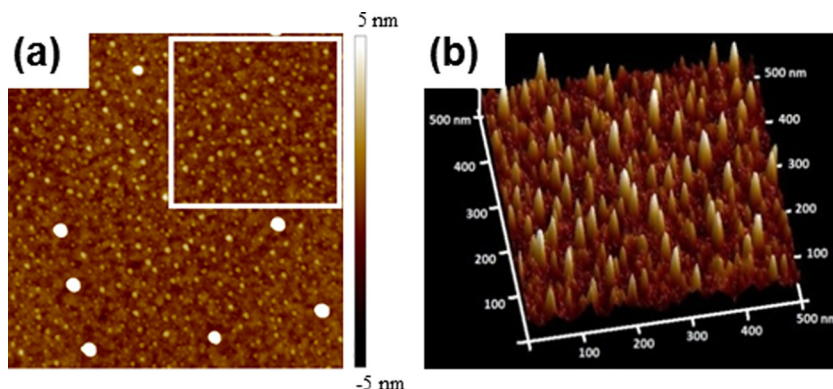


FIG. 3. (a) AFM topography image ($1 \times 1 \mu\text{m}^2$) of a gold film deposited by PLD at 213 nm and 2 J/cm^2 with 144 000 pulses on the cantilever array surface. The region selected in (a) by a white square is displayed in (b) in a 3D representation.

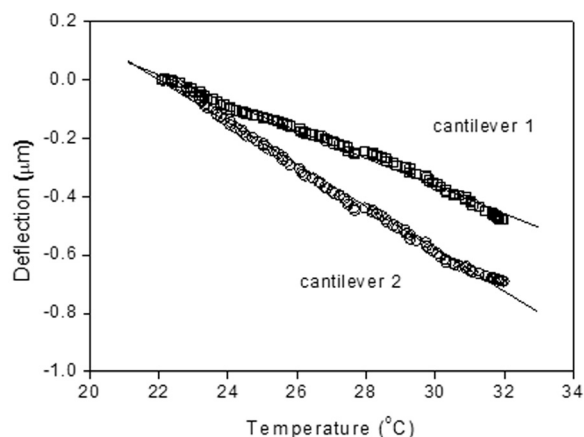


FIG. 4. Deflection of two gold-coated cantilevers as a function of temperature. The symbols (squares for cantilever 1 and circles for cantilever 2) represent experimental data and the lines correspond to linear fittings. The deflection of the micromechanical sensors was measured with respect to the deflection at the initial experimental temperature (22 °C). The temperature was changed at a rate of about 0.14 °C per minute.

gold-coated micromechanical sensors prepared by PLD. After gold coating with PLD (squares), the cantilevers experience a maximum surface stress of -0.05 ± 0.02 N/m to a RH increment of 40%. After the functionalization steps that lead to the creation of a monolayer of dsDNA on the gold surface (circles), all the cantilevers bend downwards toward the silicon side until they reach a saturation value at a RH of 50%. The mean surface stress variation out of 20 measurements is -1.00 ± 0.26 N/m. This negative change of surface stress indicates that the adsorption of DNA molecules induces a compressive stress in the gold layer, because by introducing a higher amount of water molecules (increasing humidity) the surface stress on the cantilever is raised. The obtained deviation can be related to deviations in the mechanical properties of the silicon cantilevers. For the sensors used in the experiments, the nominal thickness provided by manufacturer has a range of 0.7–1.3 μm , which may explain the differences in the measured surface stress. The results shown herein are consistent with previous reports^{17,27} where the

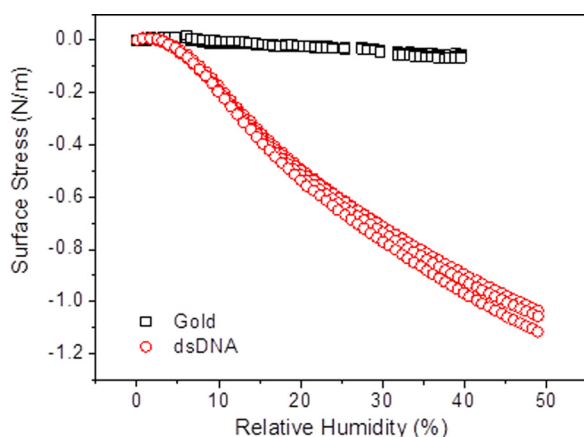


FIG. 5. Surface stress variation during a hydration cycle for five cantilevers of one gold-coated micromechanical sensor, after gold coating with PLD (squares) and after DNA hybridization (circles). The surface stress variations were measured with respect to the surface stress at RH 0%. RH was changed at a rate of about 1% per minute.

authors described a method for DNA hybridization detection based on hydration-induced tension layers.

The values of surface stress obtained for the biomechanical sensors prepared by PLD are compared with those reported¹⁷ for cantilevers coated by the more conventional technique of thermal evaporation. Using the latter technique the reported surface stress at the saturation point is -0.15 N/m,¹⁷ approximately seven times lower than the values measured herein for the sensors prepared by PLD.

IV. DISCUSSION

Gold deposits on chromium-coated silicon substrates were obtained upon irradiation at 213 nm using different number of pulses of 2 J/cm^2 in order to control their thickness and morphology and aiming at obtaining films with the optimal properties for use as DNA sensors. It was found that for a number of pulses below 12 000, very thin nanoparticle-assembled gold layer was obtained, with thickness below 3 nm and nanoparticle size from some tens of nm up to 300 nm. For a larger number of pulses, the film is continuous and displays a roughness which is lower than that of the thinner nanoparticle-assembled layers. These differences can be explained in relation to the nucleation processes of the laser ablated species that take place on the substrate. In fact, it has been proposed^{14,28,29} that defects created during layer growth by the high energetic plasma species reaching the substrate are responsible of the nucleation process. At the initial state of deposition, the dominating island-like growth results in small coverage of the surface area by clusters. When the relative area covered by nucleating and growing clusters increases, the deposition rate decreases, due to rising self-sputtering. As this effect is quite efficient at the laser fluence used, it is estimated²⁹ that only about 10% of the arriving atoms will contribute to film growth, while the rest are self-sputtered from the surface by the incoming flux. This explains the nonlinear dependence of the film thickness versus the number of pulses (Table I). Self-sputtered processes are also thought to be responsible of the evolution of the nanoparticle size.¹⁴

The presence of overimposed aggregates in the case of gold layers fabricated with a larger number of pulses (≥ 12 000) can be explained by taking into account in this case the ejection mechanism. This is dominated by explosive boiling of the target material,^{10–13} a phenomenon which is described as an explosive relaxation of the laser induced melt into a coexistent mixture of liquid droplets and vapor. When a target is irradiated by ns laser pulses, the thermal contributions generally dominate and allow photon coupling with both the electronic and vibrational modes of the material. Such effects will be most favored in cases where the target has a large absorption coefficient (thus ensuring a small optical penetration depth). At 213 nm, the absorption coefficient of gold is estimated in $\alpha \approx 8 \times 10^5 \text{ cm}^{-1}$,³⁰ and thus a thin layer of around 12 nm is heated up. The heat accumulation in this narrow layer is responsible for the explosive boiling of the target. Macroscopic particulate ejection can also contribute in the case of non-homogeneous targets, where the localized laser induced heating will cause very rapid

expansion of any trapped gas pockets, just below the surface, and forcible ejection of the surface material.¹⁰ Then, although the target is continuously rotated and linearly translated to avoid cratering, the fabrication of thicker deposits and, in particular, of 20 nm thick gold layers results in some defects on the target surface, possibly enhancing production of aggregates.

Regarding the crystallinity of the deposited gold layer, and as mentioned above, there is a preferential orientation of gold crystallites, which is related to the kinetic energy of the ejected species.²⁴ For the characteristic kinetic energies applicable to these experiments (which have been reported to be ≥ 3.0 eV in similar experimental conditions),¹⁴ the preferential orientation of the crystallites is a manifestation of a minimum in the configuration energy, as (111) surfaces have the closest packing in the face centered cubic structure adopted by gold.

The residual stress, defects, and roughness of the coatings are parameters that affect the mechanical response of the micromechanical sensors to molecular adsorption.²⁷ The analysis of the surface topography of 20 nm gold coated micromechanical sensors prepared by PLD upon 144 000 pulses proves that the obtained gold layers are continuous with a nanostructured morphology. By functionalizing PLD gold coated cantilevers with dsDNA monolayers, we have found quantitative differences in comparison to the same type of cantilevers, in terms of area, and for similar gold layer thickness (ca., 20 nm)¹⁷ when coating with thermal evaporation techniques. The induced surface stress upon hydration forces on the functionalized cantilever surface is qualitatively similar (it generates a compressive surface stress) in both cases, but around seven times higher for the PLD based procedure. Since the surface stress is proportional to the number of DNA chains on top of the gold layer, this result can be attributed to the higher capability of creating a monolayer of DNA with a higher density in the case of PLD. By tuning the PLD conditions, it is possible to increase the number of binding sites on the nanostructured gold films. A larger gold surface roughness enhances the micromechanical sensor effective area and consequently the number of molecular binding sites. In addition, surface roughness improves the confinement of molecules, increasing the intermolecular interaction, based in osmotic, steric, solvation and hydration forces, in comparison to the more uniform surfaces generated by thermal evaporation.³¹

V. CONCLUSIONS

PLD was used for gold-coating silicon cantilever arrays using the fifth harmonic of a Nd:YAG laser (213 nm, pulse duration 15 ns). Optimal irradiation parameters, fluence and number of pulses, were determined in order to obtain nanostructured gold films with a thickness of 20 nm, a value which has been previously reported to be appropriate for adequate DNA biosensor performance. The measurement of the mechanical response of the PLD coated sensors upon hydration before and after adsorption of self-assembled DNA monolayers showed that the surface stress induced by the adsorption of DNA molecules is around seven times higher than for bio-

sensors coated by other more conventional method such as thermal evaporation. This improvement of performance is attributed to the increase of superficial roughness and effective area of the nanostructured gold layer, which in turn increases the number of molecule binding sites and their confinement to the surface by stronger intermolecular interactions. These results indicate that gold-coating by PLD could be an advantageous method to enhance the response of micromechanical devices in biosensing applications.

ACKNOWLEDGMENTS

Funding from MICINN, Spain (Project CTQ2010-15680) is gratefully acknowledged. E.R. and M.S. thank MICINN (Juan de la Cierva Programme) and CAM (Geomateriales S2009/MAT 1629), respectively, for contracts. We are grateful to Professor T.A. Ezquerro (IEM, CSIC) for the use of the AFM system and M. Juanco (ICA, CSIC) for XRD measurements.

¹F. Rosei, *J. Phys.: Condens. Matter*, **16**, S1373 (2004).

²A. Vaseashta and D. Dimova-Malinovska, *Sci. Technol. Adv. Mater.*, **6**, 312 (2005).

³S. Venkatchalam, D. Soundararajan, P. Peranatham, D. Mangalaraj, S. K. Narayandass, S. Velumani, and P. Schabes-Retchkiman, *Mater. Charact.*, **58**, 715 (2007).

⁴B. D. Cullity, *Elements of X-Ray Diffraction* (Addison Wesley Publishing Company, Inc., London, 1978).

⁵A. Erdem, M. Pividori, M. del Valle, and S. Alegret, *J. Electroanal. Chem.*, **567**, 29 (2004).

⁶K. Millan, A. Saraulo, and S. R. Mikkelsen, *Anal. Chem.*, **66**, 2943 (1994).

⁷J. Wang, *Anal. Chim. Acta*, **500**, 247 (2003).

⁸D. B. Chrisey, A. Piqué, R. A. McGill, J. S. Horwitz, B. R. Ringeisen, D. M. Bubb, and P. K. Wu, *Chem. Rev.*, **103**, 553 (2003).

⁹R. Eason, *Pulsed Laser Deposition of Thin Films: Applications-Led Growth of Functional Materials* (Wiley-Blackwell, New York, 2006).

¹⁰M. Sanz, M. López-Arias, J. F. Marco, R. de Nalda, S. Amoroso, G. Ausanio, S. Lettieri, R. Bruzzese, X. Wang, and M. Castillejo, *J. Phys. Chem. C*, **115**, 3203 (2011).

¹¹M. Walczak, M. Oujja, J. F. Marco, M. Sanz, and M. Castillejo, *Appl. Phys. A: Mater. Sci. Proc.*, **93**, 735 (2008).

¹²M. Sanz, M. Walczak, M. Oujja, A. Cuesta, and M. Castillejo, *Thin Solid Films*, **517**, 6546 (2009).

¹³M. Sanz, M. E. López-Arias, E. Rebolgar, R. de Nalda, and M. Castillejo, *J. Nanopart. Res.*, **13**, 6621 (2011).

¹⁴J. Gonzalo, A. Perea, D. Babonneau, C. N. Afonso, N. Beer, J.-P. Barnes, A. K. Petford-Long, D. E. Hole, and P. D. Townsend, *Phys. Rev. B*, **71**, 125420 (2005).

¹⁵M. Godin, V. Tabard-Cossa, Y. Miyahara, T. Monga, P. J. Williams, L. Y. Beaulieu, R. B. Lennox, and P. Grutter, *Nanotechnology*, **21**, 075501 (2010).

¹⁶D. Ramos, J. Mertens, M. Calleja, and J. Tamayo, *Sensors*, **7**, 1757 (2007).

¹⁷J. Mertens, C. Rogero, M. Calleja, D. Ramos, J. A. Martín-Gago, C. Briones, and J. Tamayo, *Nat. Nanotechnol.*, **3**, 301 (2008).

¹⁸W. Shu, D. Liu, M. Watari, C. K. Riener, T. Strunz, M. E. Welland, S. Balasubramanian, and R. A. McKendry, *J. Am. Chem. Soc.*, **127**, 17054 (2005).

¹⁹N. F. Martínez, P. M. Kosaka, J. Tamayo, J. Ramírez, O. Ahumada, J. Mertens, T. D. Hien, C. V. Rijn, and M. Calleja, *Rev. Sci. Instrum.*, **81**, 125109 (2010).

²⁰P. M. Kosaka, J. Tamayo, E. Gil-Santos, J. Mertens, V. Pini, F. M. Martínez, O. Ahumada, and M. Calleja, *J. Appl. Phys.*, **109**, 064315 (2011).

²¹R. Raiteri, M. Grattarola, H. J. Butt, and P. Skälådal, *Sens. Actuators B*, **79**, 115 (2001).

²²J. Mertens, M. Calleja, D. Ramos, A. Tarín, and J. Tamayo, *J. Appl. Phys.*, **101**, 034904 (2007).

²³D. Y. Petrovykh, H. Kimura-Suda, L. J. Whitman, and M. J. Tarlov, *J. Am. Chem. Soc.*, **125**, 5219 (2003).

²⁴E. Irissou, B. Le Drogoff, M. Chaker, and D. Guaya, *Appl. Phys. Lett.*, **80**, 1716 (2002).

- ²⁵G. Webber, G. Stevens, F. Grieser, R. Dagastine, and D. Chan, *Nanotechnology* **19**, 105709 (2008).
- ²⁶T. W. Clyne, *Key Eng. Mater.* **116/7**, 307 (1996).
- ²⁷Mecwins patent WO/2009/053195.
- ²⁸A. Perea, J. Gonzalo, C. Budtz-Jorgensen, G. Epurescu, J. Siegel, C. N. Afonso, and J. Garcia-Lopez, *J. Appl. Phys.* **104**, 084912 (2008).
- ²⁹A. Zenkevitch, J. Chevallier, and I. Khabelashvili, *Thin Solid Films* **311**, 119 (1997).
- ³⁰E. D. Palik, *Handbook of Optical Constants of Solids* (Academic, New York, 1997).
- ³¹J. J. Headrick, M. J. Sepaniak, N. V. Lavrik, and P. G. Datskod, *Ultramicroscopy* **97**, 417 (2003).